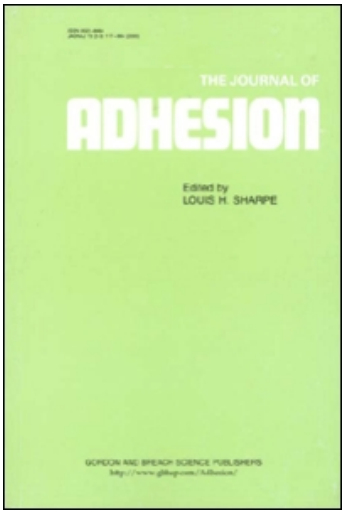

The Journal of Adhesion
Publication details, including instructions for authors and subscription information:
http://www.informaworld.com/smpp/title~content=t713453635

Experimental Parameters Controlling Adhesion of Biomimetic Fibrillar Surfaces

Christian Greiner[a]; Sebastian Buhl[a]; Aránzazu del Campo[ab]; Eduard Arzt[ab]
[a] Max Planck Institute for Metals Research, Stuttgart, Germany [b] INM-Leibniz Institute for New Materials, Campus D2 2, 66123 Saarbruecken, Germany

To cite this Article Greiner, Christian , Buhl, Sebastian , del Campo, Aránzazu and Arzt, Eduard(2009) 'Experimental Parameters Controlling Adhesion of Biomimetic Fibrillar Surfaces', The Journal of Adhesion, 85: 9, 646 — 661
To link to this Article: DOI: 10.1080/00218460902997042
URL: http://dx.doi.org/10.1080/00218460902997042

The Journal of Adhesion, 85:646–661, 2009

ISSN: 0021-8464 print/1545-5823 online
DOI: 10.1080/00218460902997042

Taylor & Francis
Taylor & Francis Group

Experimental Parameters Controlling Adhesion of Biomimetic Fibrillar Surfaces

Christian Greiner, Sebastian Buhl, Aránzazu del Campo, and Eduard Arzt
Max Planck Institute for Metals Research, Stuttgart, Germany

The recently emerging interest in fibrillar biological attachment systems, as those found in the gecko, has led to the fabrication of micropatterned elastomer adhesion surfaces. Reported studies have demonstrated that measurements on micropatterned surfaces are affected by experimental parameters not relevant for flat samples. The present paper investigates the influence on adhesion values of the sample stiffness, the backing layer thickness, the ambient humidity, and of repetitive measurements at the same location. Measurements were performed on PDMS (Sylgard® 184) micropatterned surfaces possessing flat-ended pillars with 10 μm diameter and 10 μm height. We find that adhesion increased with decreasing sample stiffness and decreasing backing layer thickness, whereas it dropped when several tests were carried out at exactly the same location. For ambient humidities between 2 and 90%, no influence on adhesion performance was found.

Keywords: Adhesion; contact mechanics; gecko adhesives; humidity; patterned surfaces

INTRODUCTION

In the science of adhesion, the testing of contact theories with rubber materials has a tradition. Johnson, Kendall, and Roberts [1] used rubber spheres to investigate the applicability of their new theory in

Received 8 December 2008; in final form 2 April 2009.
One of a Collection of papers honoring J. Herbert Waite, the recipient in February 2009 of *The Adhesion Society Award for Excellence in Adhesion, Sponsored by 3M*.
Present address of Aránzazu del Campo and Eduard Arzt is INM-Leibniz Institute for New Materials, Campus D2 2, 66123 Saarbruecken, Germany.
Address correspondence to Christian Greiner, University of Pennsylvania, 112 Towne Building, 220 South 33rd St., PA 19104, Philadelphia, USA. E-mail: greiner@mf.mpg.de

the 1970s. In the following decades, mainly poly(dimethyl siloxane) (PDMS)-based rubbers were used for such experiments, for example, by Chaudhury and Whitesides [2] in 1991. Recently, the fibrillar attachment organs found in geckos [3,4] and other animals [5–7] inspired numerous studies on (micro-)patterned PDMS surfaces. Such tests were either performed in peeling [8,9] or in nominally perpendicular adhesion tests [10–17]. In these studies it was found that adhesion of fibrillar surfaces is a function of preload [14,18], a dependence not found with flat samples. Also, a strong influence of fiber tip shape [11,18,19] and pillar diameter [10,14] was reported. In order to ensure the reproducibility of such results and to allow their unambiguous interpretation, several experimental parameters have to be well controlled. This paper aims to shed light on the influence of parameters which have been neglected so far: Young's modulus, backing layer thickness, exact location of the measurements, and ambient humidity. Experiments were carried out on PDMS surfaces with pillars of 10 μm radius and an aspect ratio of 1, extending earlier studies with the same material and methods [11,14]. To achieve reliable adhesion data, it is essential to take these additional effects into account.

EXPERIMENTAL

Arrays of PDMS flat-ended micro pillars were obtained by soft-molding Sylgard® 184 on arrays of holes made by lithographic patterning of thick SU-8 films (and epoxy-based negative tone photoresist for the fabrication of high aspect ratio structures), as previously reported [14,20,21]. The dimensions of fabricated pillars were 10 μm in radius and 10 μm in height, giving an aspect ratio, λ, of 1 in all cases. The interpillar distance was identical to the pillar diameter and the packing geometry was hexagonal, resulting in a pillar packing density of 22.7%. Silicon wafers (100 orientation) were provided by Crystec (Berlin, Germany). SU-8 type 25 and the developer mr-Dev 600 were provided by Micro Resist Technology (Berlin, Germany). Hexadecafluoro-1,1,2,2,-tetrahydrooctyltrichlorosilane was purchased from ABCR (Karlsruhe, Germany). Masks for lithography were provided by ML&C (Jena, Germany) or quartz with $0.8 \times 0.8\,cm^2$ chrome patterned fields. A mask aligner, Karl Suss MJB3 (Garching, Germany), was used for the irradiation step. Sylgard 184 was purchased from Dow Corning (Midland, MI, USA). The profiles of the patterned surfaces were characterized by interferometry using a ZYGOLOT 5000 equipment (Middlefield, CT, USA) and by scanning electron microscopy using a LEO 1530VP (Oberkochen, Germany).

Soft-Molding

A 10:1 ratio of Sylgard® 184 prepolymer and crosslinker was mixed, degassed, and poured on a silanized SU-8 patterned wafer (see reference [14] for more details). For standard samples, curing for 14 hours at 65°C in light vacuum (~600 mbar) afforded accurate replicas. The total thickness of the elastomer samples was controlled with a Teflon® ring of defined height which surrounded the wafer. Standard samples had a sample thickness of 5 mm. For each set of experiments, the same SU-8 master was used for molding in order to guarantee identical geometry of the replicated structures. Samples with backing thickness varying from 0.54 to 28.06 mm were obtained by using Teflon® rings with variable heights. The final thickness was measured with a micrometer caliper after curing. In order to fabricate PDMS surfaces with higher stiffness, an additional post-curing step at 150°C for up to 50 h was performed before demolding. The exact curing conditions for these samples can be found in Table 1.

Adhesion Measurements

The adhesion performance of the hexagonal-patterned surfaces was tested by recording load-displacement curves obtained with a home-built indentation equipment [11,14,22]. This apparatus consists of a glass spring mounted on a piezoelectric crystal (P-611 NanoCube, Physik Instrumente, Karlsruhe, Germany) and coupled to a hexapod

TABLE 1 Curing Conditions for Micropatterned PDMS Samples with Different Effective Young's Moduli E^*

Reduced Young's modulus E^* (MPa)	Curing time (h)
0.83	14 h 02 min at 65°C
0.89	14 h 41 min at 65°C
0.91	14 h 42 min at 65°C
0.97	14 h 41 min at 65°C + 14 h 42 min at 65°C
1.16	14 h 00 min at 65°C + 2 h 17 min at 150°C
1.20	14 h 02 min at 65°C + 50 h 33 min at 150°C
1.23	14 h 29 min at 65°C + 24 h 08 min at 150°C

The values were obtained by fitting the compressive parts of the load-displacement curves with Eq. (1). The error for E^* is below 0.01 MPa.

nanopositioning stage (F-206, Physik Instrumente, Karlsruhe). A sapphire sphere with a diameter of 5 mm (Goodfellow, Huntingdon, U.K.) was glued to the free end of the glass spring. Using a spherical tip solved the problem of possible misalignment between probe and surface occurring in flat-flat contacts. The patterned sample was placed on the positioning stage and the sphere was brought in contact. After compressive preloading, the sphere was retracted at a constant rate of 1 μm/s until pull-off occurred. The maximum vertical displacement of the piezo was 100 μm and the positioning accuracy was 1 nm. The stage had a maximum travel range of 12 mm with an accuracy of 100 nm. Spring deflection during contact was monitored *via* a laser interferometer (SP 120, SIOS, Ilmenau, Germany). Calibration of the spring allowed conversion of the deflection into force. Using a spring with stiffness 130 N/m, forces up to 4 mN could be measured with a resolution of 1 μN. For tests performed with controlled ambient humidity, a four-leaf force sensing spring was installed in the equipment. More details on this spring design can be found in Ref. [23]. The spring had a stiffness of 309 N/m and somewhat higher absolute adhesion values were found than with the double-leaf cantilevers usually employed. This was due to the slight non-linearity of the latter setup [23]. Data collection was performed with a Labview software package (Austin, TX, USA). The sapphire sphere was cleaned with high-purity ethanol before each test.

Since the mechanical properties of polymers may change over time, all adhesion experiments were performed immediately after fabrication without any further aging of the sample. The laboratory temperature and humidity were registered for each measurement with a P 330 tool (Tematec, Hennef, Germany). In standard conditions, the temperature during the experiments was ~23°C and the humidity ~26%. A minimum of five measurements was performed for each data point. For comparison, adhesion tests under the same conditions were also conducted with flat specimens (data not shown here). For measuring the adhesion properties under different ambient humidities, the entire testing setup was encapsulated with a PMMA box. The box was either flushed with dry nitrogen or with nitrogen being pressed through water in a washing flask at different flow rates. For humidities exceeding 60%, the water was heated up to about 90°C. The accuracy of this method was within 2% in relative humidity. Before starting an adhesion experiment, the humidity was equilibrated for 1 hour. For measuring the evolution of the adhesion properties after repetitive measurements at the same position, additional force–displacement curves were determined 1, 2, 3, 4, 18, and 19 hours after the first measurement.

RESULTS AND DISCUSSION

A representative SEM picture showing the quality of our samples is presented in Fig. 1. The patterned fields ($0.8 \times 0.8\,\mathrm{mm}^2$) were defect-free, as required for reproducible measurements. The adhesion properties of freshly prepared samples with different Young's moduli and different backing thicknesses were measured at controlled experimental conditions, as specified in the experimental section. Additionally, measurements at different humidity conditions were performed. The results are presented and discussed in the following sections.

Young's Modulus Effect

Seven samples with different Young's moduli were obtained by post-curing the PDMS material for increasing times. The moduli were obtained by fitting the compressive parts of the load-displacements curves to the Hertzian expression [24]:

$$P = \frac{4}{3} E^* \sqrt{R\delta^3}, \tag{1}$$

where P is the applied compressive preload, R the radius of the indenting sphere, δ the indentation depth, and $E^* = E/(1-\nu^2)$ the reduced Young's modulus, with $\nu = 0.5$ as Poisson's ratio. Reduced Young's moduli between $E^* = 0.83$ and 1.23 MPa were obtained.

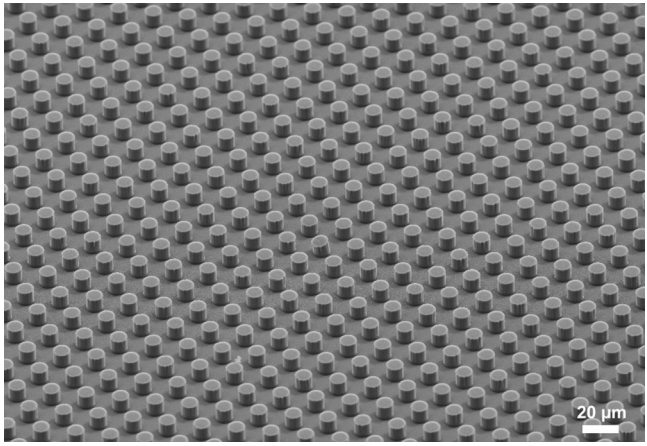

FIGURE 1 SEM micrograph of a PDMS test surface structured with 10 µm radius pillars having an aspect ratio of 1 (hexagonal packing, packing density 22.7%). The specimen was coated with 10 nm of Au/Pd for SEM observation.

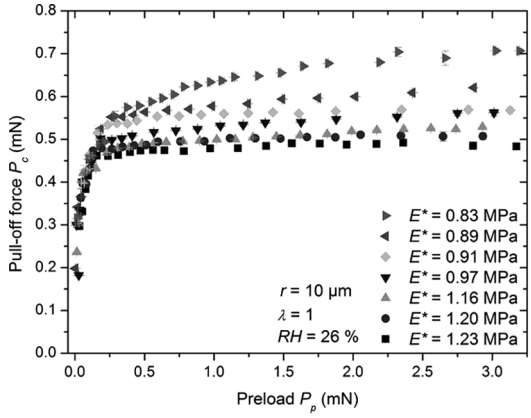

(a)

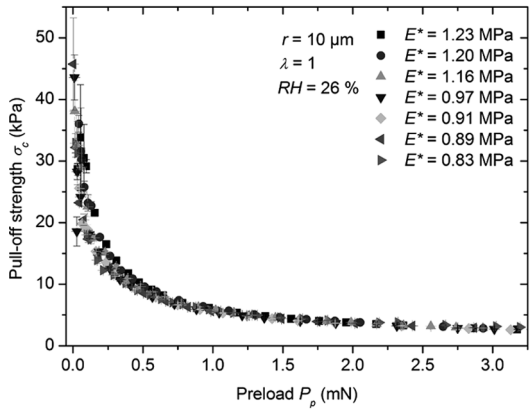

(b)

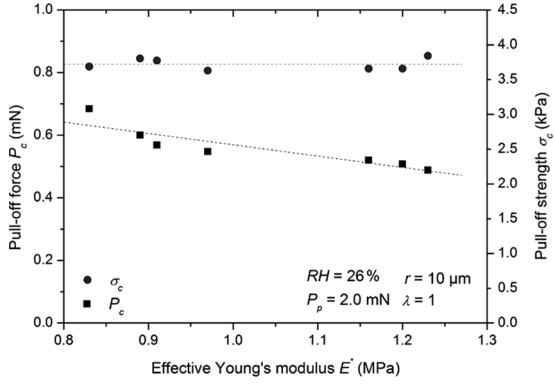

(c)

Figure 2a shows the measured pull-off forces, P_c, plotted *versus* the applied preload, P_p, for the different samples. P_c corresponds to the force at the final detachment event. As described in earlier publications [14,18], P_c values of structured surfaces vary with preload when using a spherical indenter and, therefore, measurements at various preload values are required to describe the adhesion performance. In Fig. 2b, the same data are plotted as the pull-off strength, σ_c, as a function of preload. The pull-off strength was evaluated by dividing the pull-off force by the apparent contact area of the indenting sphere with the patterned surface, at maximum preload [14]. This quantity is a meaningful parameter to compare different adhesives.

According to the results obtained, the pull-off force of the structured surfaces decreased with increasing PDMS stiffness (see Fig. 2c, which shows P_c and σ_c as a function of effective Young's modulus). A drop by a factor of 1.4 (from $P_c = 0.68$ to 0.49 mN) was measured when the effective Young's modulus was increased 1.5 fold ($E^* = 0.83$ to 1.23 MPa). These results contradict the classic JKR model [1] for the pull-off force of a sphere from a flat substrate, which is given by

$$P_c = \frac{3}{2}\pi\gamma R^*, \tag{2}$$

where γ is the work of adhesion and R^* the relative radius of curvature. According to Eq. (2), the Young's modulus should not affect the pull-off force at all (within the limits of JKR theory).

Taking into account that in our experiments the sphere (diameter of 5 mm) is much bigger than the PDMS pillars (diameter of 20 μm), one could assume the contact geometry to be described approximately by the contact of flat punches with a planar surface. This contact problem was solved by Kendall [25], giving the following pull-off force for a punch of radius r:

$$P_c = \sqrt{8\pi\gamma E^* r^3}. \tag{3}$$

According to Eq. (3), the pull-off force should increase with increasing effective Young's modulus, in direct contradiction to our experimental

FIGURE 2 Effect of Young's modulus on adhesion (pillars of radius $r = 10\,\mu m$ and aspect ratio $\lambda = 1$). The samples had different reduced Young's moduli, which were obtained through different curing conditions (the exact curing temperatures and times are given in Table 1. (a) Pull-off force *vs.* preload, (b) pull-off strength σ_c (force per apparent contact area) *vs.* preload, (c) pull-off force and strength *vs.* effective Young's modulus (at a preload of 2 mN). The broken lines were obtained through a linear fit to the data.

results. The fact that Eq. (3) was derived for the contact of a stiff punch against an elastic substrate—the opposite of our contact pair, where the PDMS pillars are more compliant than the sapphire sphere—does not explain the contradiction. Spolenak *et al.* [26] argued that Eq. (3) may also be valid for elastic pillars against a stiff substrate (within 10% accuracy). It is more likely that the decreasing adhesion force with increasing stiffness is due to surface roughness. Roughness of the PDMS pillars can be neglected as they were molded against a flat silicon wafer; however, the surface roughness of the sapphire sphere has to be considered, even though a polished quality was used for the experiments. Fuller and Tabor [27] demonstrated in 1975 that an increase in modulus increases the sensitivity to surface roughness and decreases the adhesion performance significantly. Similar results were found by Peressadko *et al.* [22] for PDMS lenses in contact with epoxy substrates of different roughnesses. Luan and Robbins argued that elastomers can deform like fluids between the crosslink spacing [28], allowing them to conform to surface roughness. With increasing stiffness, the spacing between the crosslinking points will decrease, leading to a reduction in P_c. For fibrillar surfaces Hui *et al.* [29] found numerically that the adhesion force also decreased with increasing fibrillar stiffness.

Figures 2b and c show that the pull-off strength as a function of preload is constant for all samples regardless of their effective Young's modulus. The decrease in the pull-off force with increasing modulus is apparently offset by a concomitant drop in contact area. The pull-off strength, being the ratio between the two, therefore remains constant.

Thickness of the Backing Layer

The influence of the total backing layer thickness on the pull-off force is demonstrated in Fig. 3a and b. P_c drops weakly with increasing backing thickness. This is surprising, as one would expect that a thicker backing layer promotes the adaptation to surface roughness, as well as the ability of the fibers to make contact due to an increase in effective compliance. This does not seem to be the case. Table 2 demonstrates that the effective Young's modulus of the structured surfaces, as determined by fitting with Eq. (1), does not change with the backing thickness. On the contrary, the elastic modulus of the flat control samples increased with thickness. At this point it has to be mentioned that in our analysis for the effective Young's modulus, no confinement effects [30] were taken into account. For the above discussion of Young's modulus effects, this was not necessary as the sample

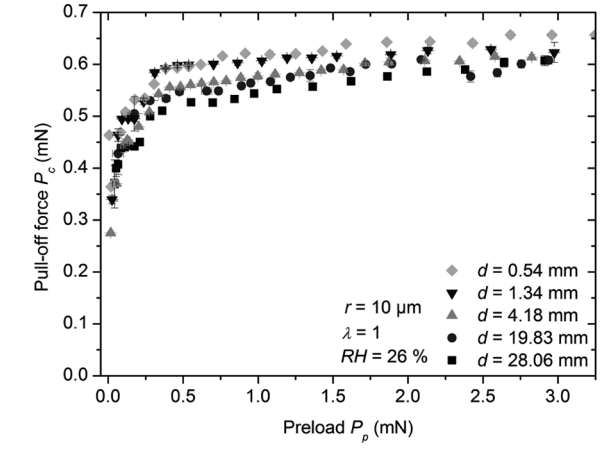

(a)

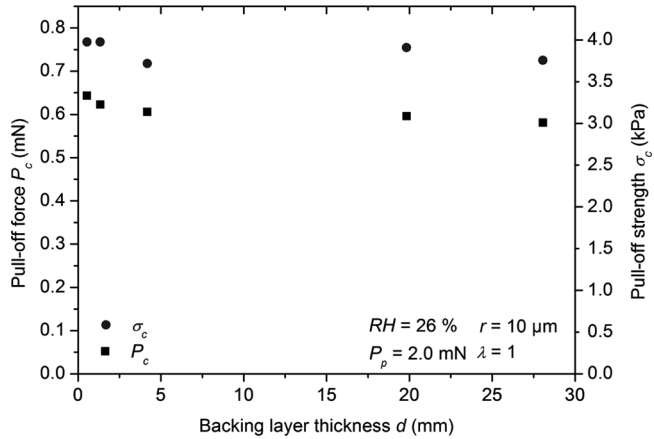

(b)

FIGURE 3 Effect of backing layer thickness: the samples had five different total thicknesses. (The reduced Young's moduli for these samples are given in Tables 2 and 3.) (a) Plotted as pull-off force *vs.* preload, (b) pull-off force and strength *vs.* backing layer thickness (at a preload of 2 mN).

thickness (5 mm) was about a factor of 25 larger than the average contact area (2×10^{-4} m). For the discussion in this paragraph, we have to take confinement effects into account and present the corrected results in Table 3. As this table demonstrates, confinement effects change the trend: Young's modulus decreases with film thickness; the behavior one would intuitively expect.

TABLE 2 Reduced Young's Moduli for Micropatterned PDMS Samples Having Different Total Thicknesses

Thickness (mm)	Reduced Young's modulus (MPa)	Reduced Young's modulus (flat sample) (MPa)
0.54	0.89	2.29
1.34	0.95	2.29
4.18	0.89	2.39
19.83	0.95	2.11
28.06	0.95	2.75

The E^* values were obtained by fitting the compressive parts of the load-displacement curves with Eq. (1). The error for E^* is below 0.01 MPa.

Kim *et al.* [31] found a similar effect for the influence of backing layer thickness on adhesion when measuring mushroom-terminated polyurethane pillars with backing thickness between 160 and 1120 μm against a flat silicon disk. For this seven-fold decrease in thickness they found an increase in pull-off force by about a factor of 9. They attributed these differences to a more effective "equal load sharing" between the fibers, with thin backing layers. In our study, the backing layer thickness was decreased by a factor of 50, whereas the increase in pull-off force was only 1.1-fold ($P_c = 0.58$ to 0.64 mN at $P_p = 2.0$ mN). This weak dependence might be due to the thicker backing layers in comparison with Kim *et al.* Very thin layers might be necessary to approach the limit of equal load sharing, a hypothesis supported by the fact that the highest gain in pull-off force was reported for the thinnest sample [31]. Unfortunately, we could not perform experiments with thinner backings because tearing of the

TABLE 3 Reduced Young's Moduli for Micropatterned PDMS Samples Having Different Total Thicknesses

Thickness (mm)	Reduced Young's modulus (MPa)	Reduced Young's modulus (flat sample) (MPa)
0.54	1.39	3.57
1.34	1.14	2.76
4.18	0.95	2.54
19.83	0.96	2.14
28.06	0.96	2.77

The E^* values were obtained by fitting the compressive parts of the load-displacement curves with Eq. (1) and taking into account confinement effects [40]. The error for E^* is below 0.01 MPa.

PDMS film occurred during peel-off. Another reason for the smaller influence of backing thickness in our samples may be found in the spherical indenter geometry, preventing equal load sharing between the fibers. In addition, Kim *et al.* investigated mushroom-shaped pillars and not flat punch terminated fibers [11]. We cannot predict at this point if this is relevant for the differences between the reported data.

The pull-off strength does not show as much dependence on backing layer thickness, as can be seen in Fig. 1a and 3b. This may be attributed to the different indentation resistances of the samples. Higher pull-off forces are accompanied by larger contact areas so that the quotient of the two of them—the pull-off strength—is more or less constant for all sample thicknesses investigated.

Repetitive Measurements at the Same Location

Figures 4a and b show that the pull-off force varies with the number of measurements at a defined position. A drop in P_c by a factor of 0.82 was detected after five measurements ($P_c = 0.88$ to $0.72\,\text{mN}$ for $P_p = 2.0\,\text{mN}$). About 50% of this reduction was recovered ($P_c = 0.80$ for $P_p = 2.0\,\text{mN}$) when the sample was not measured for 14 hours. After this recovery time, the same trend was observed in new measurements at the same location. Interestingly, similar trends were found for the pull-off strength (Fig. 4b). The complete σ_c-P_P-plot can be found Fig. 2a.

This behavior is rather surprising, as we expected a purely elastic behavior of our material [32] with instantaneous recovery and, therefore, a constant value of P_c independent of the number of measurements. However, it has been reported that commercial Sylgard 184 contains oligomers and rings which do not take part in the crosslinking reaction [33,34]. They are thought to diffuse between the crosslinking sites during loading and have been made partially responsible for the considerable contact angle recovery of electrically discharged PDMS [33]. We now speculate that the contribution of these molecules to the adhesion is lost as they are effectively expelled from the contact area over time when repeated indentation events take place at the same position (like water out of a hydrogel). When the sample is left to relax for longer times, the molecules may diffuse back to the contact area and contribute again to the adhesion in a subsequent indentation experiment. In control measurements, where the location for each test was varied, a constant adhesion value was found for all tests, as expected and in agreement with our hypotheses.

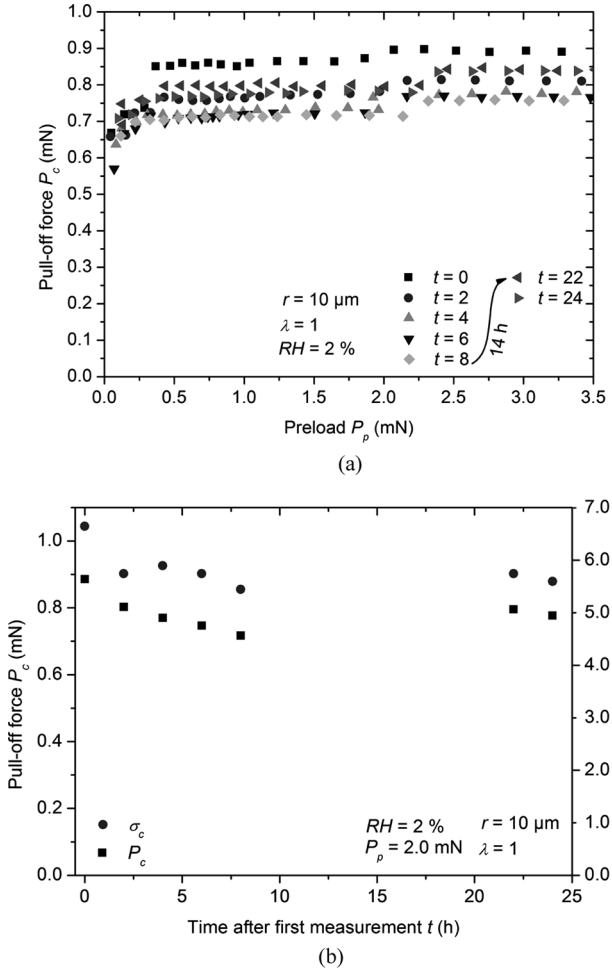

FIGURE 4 Effect of repetitive measurements at the same location after t hours following the first experiment: between test, 5 and 6 was a waiting time of 14 h. (a) Pull-off force *vs.* preload, (b) pull-off force and strength *vs.* time after first measurement (at a preload of 2 mN).

Humidity Effect

The influence of ambient humidity on pull-off force and strength at different preloads is shown in Figs. 5a and b (see Fig. 3a for the σ_c-P_P-plot). The plots illustrate that the adhesion of the micropatterned PDMS surfaces is not influenced by ambient humidity (even for changes between 2 and 90%). This behavior can be explained by

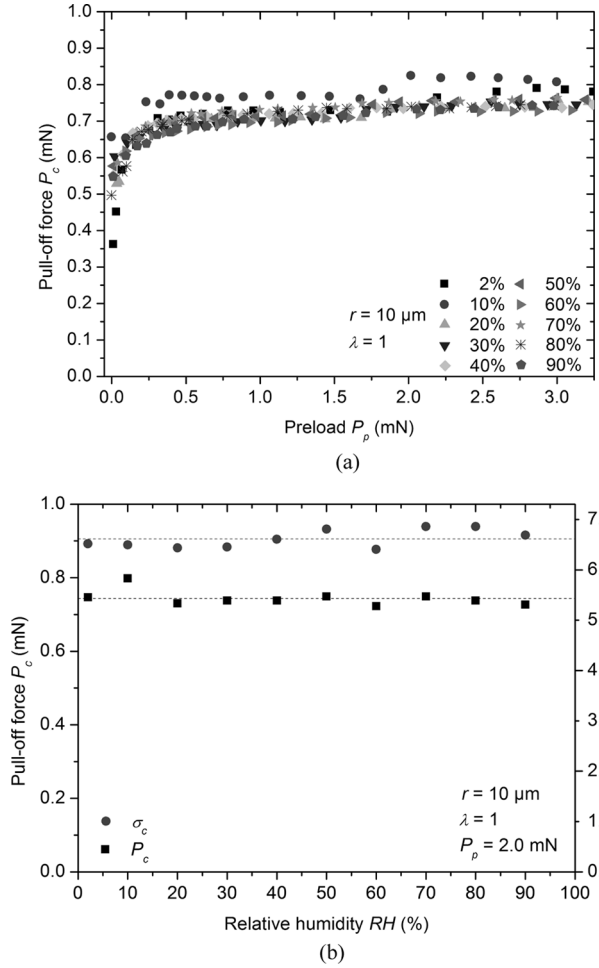

FIGURE 5 Effect of ambient humidity: pull-off force and strength at ten different ambient humidities between 2 and 90%. The humidity was equilibrated for 1 h. (a) Plotted as pull-off force *vs.* preload; (b) pull-off force and strength *vs.* relative humidity (at a preload of 2 mN). The broken lines indicate the mean average for P_c and σ_c.

the hydrophobic nature of PDMS (water contact angle ~108°). It will, thus, not attract condensed water vapor from the ambient to form meniscus bridges and will not cause any capillary forces to contribute to adhesion. In the literature, such contributions have been made responsible for increasing adhesion of plasma-treated PDMS [35] with humidity. For untreated PDMS the authors found a behavior very

similar to the one reported here. It is important to note that the literature seems inconsistent when it comes to the humidity effect on adhesion even for similar contact pairs [35–42]. Some authors [36–38,41,42] report an increase in adhesion, some a decrease [40], and others found constant values [38,41,42] with increasing humidity. Interestingly, for single gecko spatulae in contact with a hydrophilic substrate possessing a similar contact angle to water as our samples, Huber *et al.* [43] found increasing pull-off forces with increasing humidity. This was attributed to a monolayer of water absorbed on the slightly rough substrate causing additional contact area [43]. Such an effect was not found with the substrates discussed on our case. It is important to note that the fibers in our samples are in the micro range (10 μm diameter), whereas the gecko spatulae investigated by Huber *et al.* were in the nanometer regime (about 200 nm). In similar experiments, we found no humidity influence on the adhesion of flat PDMS (data not shown here).

CONCLUSION

Sylgard 184 surfaces were micropatterned with flat-ended pillars of 10 μm radius and an aspect ratio of 1. The adhesion properties of these surfaces were determined with a spherical probe indenter and the influence of several experimental parameters was systematically investigated. We summarize our main findings as follows:

- **Inverse Young's modulus effect.** The pull-off force, P_c, increased with decreasing substrate stiffness. For a 1.5-fold increase in modulus, the pull-off force dropped by a factor of 1.4. This is in contrast to the classic JKR result both for a sphere and for a flat punch in contact with a plane.
- **Slight effect of backing layer thickness.** A slight increase in the pull-off force was found with decreasing total sample thickness. Changing the backing layer thickness by a factor of 50 caused the adhesion force to drop by 10%. This small effect might be explained by a more equal sharing of the load between the fibers for smaller sample thicknesses.
- **Adhesion loss in repetitive tests.** A drop in adhesion force was found when performing repetitive adhesion measurements at the same location. About 50% of this reduction was recovered when the sample was not indented for 14 hours. This suggests that for reproducible adhesion testing a new location has to be chosen each time.
- **No ambient humidity effect.** For relative ambient humidities between 2 and 90%, no influence of humidity on the pull-off force was found on our PDMS surfaces.

ACKNOWLEDGMENT

Lithography was performed in the cleanroom of the Max Planck Institute for Solid State Research; we are grateful to Prof. K. von Klitzing and M. Riek. C.G. acknowledges discussions with Dr. Emerson de Souza.

REFERENCES

[1] Johnson, K. L., Kendall, K., and Roberts, A. D., *Proc. R. Soc. London, Ser. A* **324**, 301–313 (1971).
[2] Chaudhury, M. K. and Whitesides, G. M., *Langmuir* **7**, 1013–1025 (1991).
[3] Autumn, K., Liang, Y. A., Hsieh, S. T., Zesch, W., Chan, W. P., Kenny, T. W., Fearing, R., and Full, R. J., *Nature* **405**, 681–685 (2000).
[4] Autumn, K. and Peattie, A. M., *Integr. Comp. Biol.* **42**, 1081–1090 (2002).
[5] Niederegger, S., Gorb, S., and Jiao, Y. K., *J. Comp. Physiol. A* **187**, 961–970 (2002).
[6] Gorb, S. N., *Proc. R. Soc. London, Ser. B* **265**, 747–752 (1998).
[7] Gorb, S. N., *Attachment Devices of Insect Cuticle*, (Kluwer Academic Publishers, Dordrecht, 2001), pp. 135–176.
[8] Ghatak, A., Mahadevan, L., Chung, J. Y., Chaudhury, M. K., and Shenoy, V., *Proc. R. Soc. London, Ser. A* **460**, 2725–2735 (2004).
[9] Lamblet, M., Verneuil, E., Vilmin, T. A. B., Silberzan, P., and Léger, L., *Langmuir* **23**, 6966–6974 (2007).
[10] Crosby, A. J., Hageman, M., and Duncan, A., *Langmuir* **21**, 11738–11743 (2005).
[11] Del Campo, A., Greiner, C., and Arzt, E., *Langmuir* **23**, 10235–10243 (2007).
[12] Glassmaker, N. J., Jagota, A., and Hui, C. Y., *Acta Biomater.* **1**, 367–375 (2005).
[13] Glassmaker, N. J., Jagota, A., Hui, C. Y., and Kim, J., *J. Roy. Soc. Interface* **1**, 23–33 (2004).
[14] Greiner, C., Del Campo, A., and Arzt, E., *Langmuir* **23**, 3495–3502 (2007).
[15] Sitti, M. and Fearing, R. S., *J. Adhes. Sci. Technol.* **17**, 1055–1073 (2003).
[16] Thomas, T. and Crosby, A. J., *J. Adhes.* **82**, 311–329 (2006).
[17] Lee, H., Lee, B. P., and Messersmith, P. B., *Nature* **448**, 338–342 (2007).
[18] Kim, S. and Sitti, M., *Appl. Phys. Lett.* **89**, 261911 (2006).
[19] Gorb, S., Varenberg, M., Peressadko, A., and Tuma, J., *J. Roy. Soc. Interface* **4**, 271–275 (2006).
[20] Del Campo, A. and Greiner, C., *J. Micromech. Microeng.* **17**, R81–R95 (2007).
[21] Del Campo, A., Greiner, C., Álvarez, I., and Arzt, E., *Adv. Mater.* **19**, 1973–1977 (2007).
[22] Peressadko, A., Hosoda, N., and Persson, B. N. J., *Phys. Rev. Lett.* **95**, 124301 (2005).
[23] Varenberg, M., Peressadko, A., Gorb, S., Arzt, E., and Mrotzek, S., *Rev. Sci. Instrum.* **77**, 066105 (2006).
[24] Hertz, H., *J. Reine Angew. Math.* **92**, 156–171 (1882).
[25] Kendall, K., *J. Phys. D-Appl. Phys.* **4**, 1186–1195 (1971).
[26] Spolenak, R., Gorb, S., Gao, H. J., and Arzt, E., *Proc. R. Soc. London, Ser. A* **461**, 305–319 (2005).
[27] Fuller, K. N. G. and Tabor, D., *Proc. R. Soc. London, Ser. A* **345**, 327–342 (1975).
[28] Luan, B. Q. and Robbins, M. O., *Nature* **435**, 929–932 (2005).
[29] Hui, C. Y., Glassmaker, N. J., and Jagota, A., *J. Adhes.* **81**, 699–721 (2005).
[30] Shull, K. R., *Materials Science and Engineering R* **36**, 1–45 (2002).

[31] Kim, S., Sitti, M., Hui, C. Y., Long, R., and Jagota, A., *Appl. Phys. Lett.* **91**, 161905 (2007).
[32] Carrillo, F., Gupta, S., Balooch, M., Marshall, S. J., Marshall, G. W., Pruitt, L., and Puttlitz, C. M., *J. Mater. Res.* **20**, 2820–2830 (2005).
[33] Kim, J., Chaudhury, M. K., and Owen, M. J., *J. Colloid Interface Sci.* **293**, 364–375 (2006).
[34] Schmid, H. and Michel, B., *Macromolecules* **33**, 3042–3049 (2000).
[35] Bhushan, B. and Cichomski, M., *J. Vac. Sci. Technol. A* **25**, 1285–1293 (2007).
[36] Bhushan, B. and Dandavate, C., *J. Appl. Phys.* **87**, 1201–1210 (2000).
[37] Ata, A., Rabinovich, Y. I., and Singh, R. K., *J. Adhes. Sci. Technol.* **16**, 337–346 (2002).
[38] Fukunishi, A. and Mori, Y., *Adv. Powder Technol.* **17**, 567–580 (2006).
[39] Asay, D. B. and Kim, S. H., *J. Chem. Phys.* **124**, 174712 (2006).
[40] Pohlmann, K. and Gahr, K. H. Z., *Materialwiss. Werkstofftech.* **31**, 280–289 (2000).
[41] Turq, V., Ohmae, N., Martin, J. M., Fontaine, J., Kinoshita, H., and Loubet, J., *Tribol. Lett.* **19**, 23–28 (2005).
[42] Hoffmann, B. and Kubier, B., *Chem. Ing. Tech.* **75**, 742–749 (2003).
[43] Huber, G., Mantz, H., Spolenak, R., Mecke, K., Jacobs, K., Gorb, S. N., and Arzt, E., *Proc. Natl. Acad. Sci. U.S.A.* **102**, 16293–16296 (2005).